In vivo demonstration that α-synuclein oligomers are toxic

Beate Winner[a,b,1], Roberto Jappelli[a,1], Samir K. Maji[c,1], Paula A. Desplats[d], Leah Boyer[a,e], Stefan Aigner[a], Claudia Hetzer[a], Thomas Loher[a], Marçal Vilar[a,2], Silvia Campioni[c], Christos Tzitzilonis[a], Alice Soragni[c], Sebastian Jessberger[a,f], Helena Mira[a,2], Antonella Consiglio[a,3], Emiley Pham[d], Eliezer Masliah[d], Fred H. Gage[a,4,5], and Roland Riek[a,c,4,5]

[a]Salk Institute for Biological Studies, La Jolla, CA 92037; [b]Junior Research Group III, Interdisciplinary Center for Clinical Research, Nikolaus-Fiebiger Center for Molecular Medicine, Friedrich-Alexander-Universität Erlangen-Nürnberg, 91054 Erlangen, Germany; [c]Laboratory of Physical Chemistry, Eidgenössische Technische Hochschule Zurich, 8093 Zurich, Switzerland; [d]Department of Neurosciences and Department of Pathology and [e]Biomedical Science Graduate Program, University of California at San Diego, School of Medicine, La Jolla, CA 92093; and [f]Institute of Cell Biology, Eidgenössische Technische Hochschule Zurich, 8093 Zurich, Switzerland

Contributed by Fred H. Gage, January 25, 2011 (sent for review December 2, 2010)

The aggregation of proteins into oligomers and amyloid fibrils is characteristic of several neurodegenerative diseases, including Parkinson disease (PD). In PD, the process of aggregation of α-synuclein (α-syn) from monomers, via oligomeric intermediates, into amyloid fibrils is considered the disease-causative toxic mechanism. We developed α-syn mutants that promote oligomer or fibril formation and tested the toxicity of these mutants by using a rat lentivirus system to investigate loss of dopaminergic neurons in the substantia nigra. The most severe dopaminergic loss in the substantia nigra is observed in animals with the α-syn variants that form oligomers (i.e., E57K and E35K), whereas the α-syn variants that form fibrils very quickly are less toxic. We show that α-syn oligomers are toxic in vivo and that α-syn oligomers might interact with and potentially disrupt membranes.

Parkinson disease (PD) is the most common movement disorder, currently affecting approximately 2% of the population older than age 60 y. Prominent neuropathological hallmarks of PD are the loss of dopaminergic neurons in the substantia nigra (SN) region of the midbrain (1) and the presence of α-syn–containing intracellular inclusions: Lewy bodies (LBs) and Lewy neurites (2). α-Syn, a 140-aa protein physiologically found in presynaptic terminals of neurons, is the major fibrillar protein in LBs and Lewy neurites in sporadic and inherited PD. Moreover, point mutations (A53T, A30P, E46K) and gene multiplications of human WT (hWT) α-syn are related to rare familial autosomal-dominant forms of early-onset PD (3–6), suggesting that increased gene dosage and aberrant protein structure may accelerate disease onset and progression.

Recent reports indicate that the accumulation of α-syn can result in the formation of intermediate-state oligomers, and oligomers of different shapes and sizes have been described (7–10). These oligomers interact with lipids, disrupt membranes (7, 8), and cause cell death in vitro (10, 11) and in nonmammalian models, such as *Caenorhabditis elegans* and *Drosophila melanogaster* (12). However, we are aware of no previous direct in vivo demonstration of the toxicity of α-syn oligomers in mammals.

We aim to establish a model that allows specific testing of the effects of α-syn oligomerization in vitro and in vivo. To elucidate the causal structure–toxicity relationship of these oligomeric protein assemblies in a mammalian system, we designed "conformation-trapped" mutants based on structural modeling of α-syn fibrils (13, 14). Structurally, amyloid fibrils of α-syn are composed of cross-β-sheets (15). Residues from approximately 30 to 110 of α-syn form the core of the fibrils, whereas the approximately 30 N-terminal residues are heterogeneous and the approximately 30 C-terminal residues are flexible (13, 14, 16, 17). Based on our structural model, recently developed from NMR data, the core of α-syn fibrils comprises five β-strands reminiscent of a five-layered "β-sandwich" (14). Several loops adjacent to and between the strands are conserved pseudorepeats containing both Lys and Glu side chains (i.e., K^{32}TKEG ^{36} N-terminal to the proposed β1, K^{43}TKEG^{47} between β1 and β2, E^{57}KTKEQ^{62} between β2 and β3, and K^{80}TVEG^{84} between β4 and β5, respectively). A salt bridge between D23 and K28 in a loop connecting two β-strands has been observed for Aβ(1–42) amyloid fibrils, and point mutations therein inhibit the formation of Aβ (1–42) fibrils (18, 19).

We hypothesized that, similar to the Aβ(1–42) amyloid protein, disruption of α-syn–specific salt bridges might affect the structure and toxicity of α-syn. Accordingly, we designed mutations with the purpose of interfering with fibril formation and produced α-syn variants that specifically form oligomers but not fibrils; we show that the ability of α-syn to form oligomers in vitro is accompanied by increased in vivo toxicity.

Results

Design and in Vitro Aggregation of hWt α-Syn and α-Syn Variants. To be able to investigate α-syn–dependent oligomer toxicity in vivo, we searched for oligomer-forming mutants. Therefore, we investigated the salt bridges between the β-strands of α-syn, specifically testing whether the introduction of Glu-to-Lys mutations at positions 35, 46 (E46K is a familial variant), 57, 61, and 83, which would prevent the formation of such salt bridges, might interfere with the formation of α-syn amyloid fibrils. By using recombinant α-syn from preparations that followed an established purification procedure (17) but omitted the precipitation step by streptomycin sulfate (protocol B), we found that the α-syn single-point mutants E35K and E57K showed a strongly decreased tendency to form fibrils compared with hWT α-syn, as evidenced by time-resolved amyloid formation measured by thioflavin T (Thio-T) binding (Fig. S1*A*). Neither variant E35K nor E57K showed EM-visible amyloid fibrils even after 1 y of incubation, but they formed very pronounced ring/pore-like structures (Fig. 1*A*). In contrast, hWT α-syn and the familial α-syn variants (A30P, E46K, and A53T) formed amyloid fibrils as expected (Fig. 1*A*). By using a more rigorous purification protocol (protocol A) that included a streptomycin sulfate precipitation step (*Materials and Methods* and *SI Materials and Methods*), we found that both E57K and E35K variants formed

Author contributions: B.W., R.J., S.A., E.M., F.H.G., and R.R. designed research; B.W., R.J., S.K.M., P.A.D., L.B., S.A., C.H., T.L., M.V., S.C., C.T., S.J., H.M., A.C., and E.P. performed research; S.K.M., S.C., and A.S. contributed new reagents/analytic tools; B.W., R.J., S.K.M., P.A.D., E.P., E.M., and R.R. analyzed data; and B.W., S.K.M., F.H.G., and R.R. wrote the paper.

The authors declare no conflict of interest.

Freely available online through the PNAS open access option.

[1]B.W., R.J., and S.K.M. contributed equally to this work.

[2]Present address: Area de Biología Celular y Desarrollo, Instituto de Salud Carlos III, 28220 Majadahonda-Madrid, Spain.

[3]Present address: Institute of Biomedicine of the University of Barcelona, 08028 Barcelona, Spain.

[4]F.H.G. and R.R. contributed equally to this work.

[5]To whom correspondence may be addressed. E-mail: gage@salk.edu or riek@salk.edu.

This article contains supporting information online at www.pnas.org/lookup/suppl/doi:10.1073/pnas.1100976108/-/DCSupplemental.

amyloid fibrils with similar efficiency as the A53T variant (Fig. S1 *B–D*, protocol A). However, when the monomer fractions, relative to size exclusion chromatography (SEC) profiles obtained from streptomycin sulfate-precipitated protein preparations (protocol A), were used as starting material and subjected to time-resolved aggregation of α-syn, only the E57K and E35K variants formed oligomer peaks at the void volume at days 5 and 10 (Fig. 1*B*). The EM images in Fig. 1*C* show the oligomers from the SEC fractions of Fig. 1*B*. They appear to be of a monodispersed nature with an estimated size of 100 nm, as measured by dynamic light scattering, which is in agreement with the literature (Fig. S1*E*) (20).

We compared these oligomers to the fibril-promoting variant α-syn(30–110), which includes the amyloid core residues from approximately 30 to 110 but lacks the aggregation-interfering C-terminal and N-terminal residues of α-syn ($n \sim 30$) (14). Indeed, α-syn(30–110) shows an accelerated growth of fibril formation compared with hWT α-syn (protocol A), and its fibril conformation is similar to that of hWT α-syn fibrils (Fig. 1*A*, protocol B; and Fig. S1*D*, protocol A) (14). The biophysical properties of the three artificial α-syn variants were also compared with the familial α-syn mutants A30P, A53T, and E46K. In line with previous observations (21), A30P formed amyloid fibrils more slowly and A53T formed them more quickly than hWT α-syn and E46K, respectively (Fig. S1*B*, protocol A). To further confirm the presence of oligomers by an independent method, we compared the immunoreactivity of E57K protein versus control and hWT α-syn by immunoblots with an oligomer-specific antibody (A11; protocol A, Fig. S2) (22). In comparison with hWT α-syn, a much stronger reactivity of the E57K variant to the oligomer-specific antibody A11 was detected on dot blots (Fig. S2*A*). Western blot analysis indicated that E57K (Fig. S2*B*, protocol A), and specifically the void peak of the SEC (fraction 16) of E57K recombinant protein (Fig. S2 *C* and *D*), reacted strongly with the A11 antibody at the level of α-syn oligomers (mostly dimers and pentamers; Fig. S2*E*). In the in vitro cell-free system, we have established a set of familial and structure-based mutants that cover oligomer-promoting and fibril-only states in vitro (Fig. 1), and we report here on their in vivo behavior.

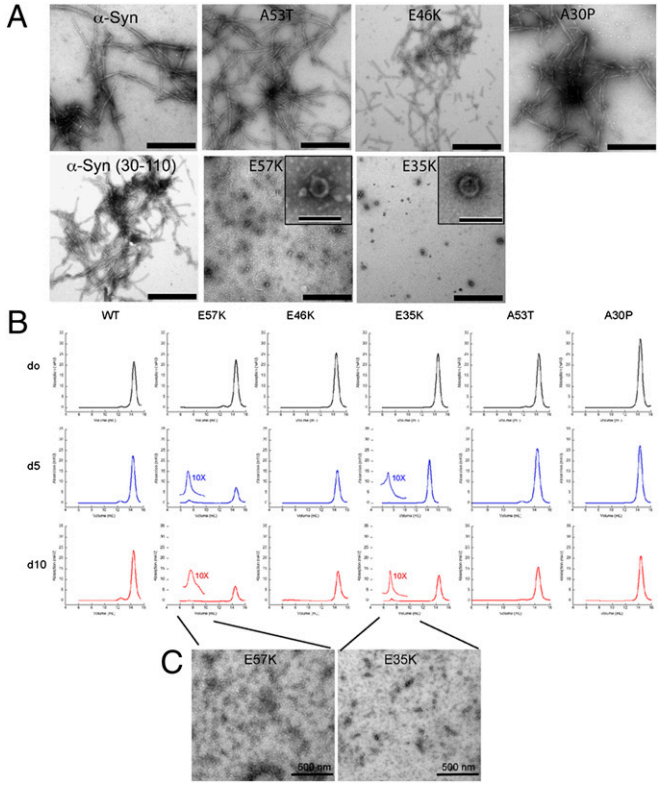

Fig. 1. In vitro aggregation of hWT α-syn and α-syn variants. (*A*) EM of aged α-syn and α-syn variants purified without the streptomycin sulfate-precipitation step (protocol B). (Scale bars: 500 nm.) *Insets*: Ring-forming entities are shown. (Scale bar: 100 nm.) (*B*) Time-resolved SEC of α-syn variants: 20 mg/mL α-syn variants were solubilized and their size exclusion profiles were measured immediately (day 0). Subsequently, after days 5 and 10, the samples of the corresponding monomer peak were again put on the SEC column, revealing that E57K and E35K had the capacity to form oligomers over time. For both α-syn variants, we show a 10-fold magnification of the oligomer peak at day 5. The decrease of the monomer peak in E35K and E57K is because they aggregate into amyloids. For the other variants and hWT α-syn, no oligomer peak was observed. (*C*) EM image of the oligomeric species from the experiment shown in *B*. (Scale bars: 500 nm.)

Toxicity of hWT α-Syn and α-Syn Variants in the SN of Lentivirus-Injected Rats. To investigate if the α-syn mutants that favor oligomer formation are more toxic in vivo than the mutants that form fibrils more quickly, the toxicity of the α-syn variants was studied in a rat model of synucleinopathies (23). This model is based on injection of lentivirus expressing the α-syn variants into the SN. Although partly limited by the fact that α-syn is overexpressed locally, it is well suited to study direct short- to medium-term toxic effects on dopaminergic neurons in an in vivo system.

Tyrosine hydroxylase (TH)-positive neurons were quantified in rats 3 wk after viral injection into the right SN and were compared with the noninjected side (Fig. 2*A*). Injections of lentivirus encoding the artificial variants E35K and E57K induced a significant loss of TH expression. The decreases in TH-positive cells for E35K was 50% (TH cell number, $2.7 \times 10^3 \pm 0.3 \times 10^3$) and 51% for E57K (TH cell number, $2.6 \times 10^3 \pm 0.2 \times 10^3$; Fig. 2 *B* and *C*) compared with the uninjected sides. These decreases for E35K and E57K were significantly different from the GFP-only group ($P < 0.001$; TH cell number, $4.6 \times 10^3 \pm 0.7 \times 10^3$). In addition, significantly fewer TH-positive cells were present in the oligomer-forming mutants E35K and E57K compared with the hWT α-syn–injected group (32% loss; TH cell number, $3.5 \times 10^3 \pm 0.2 \times 10^3$; $P < 0.05$). The faster fibril-forming mutant α-syn (30–110) did not show a significant decrease in TH-positive cell numbers (9% loss; TH cell number, $4.3 \times 10^3 \pm 0.7 \times 10^3$; $P > 0.05$ vs. GFP-only group). The data were obtained by performing cell counts for the entire SN by using a systematic, random counting procedure and comparing lesioned and unlesioned SN. The loss of TH-expressing cells caused by α-syn variant expression was more pronounced close to the injection site, as depicted in Fig. 2 *C* and *E*. We then compared these results versus the familial mutants. The rats injected with A30P (38% loss; TH cell number, $3.0 \times 10^3 \pm 0.4 \times 10^3$) and E46K (40% loss; TH cell number, $3.2 \times 10^3 \pm 0.4 \times 10^3$) did not differ significantly from those injected with E35K and E57K. A53T-injected rats (17% loss; TH cell number, $4.3 \times 10^3 \pm 0.3 \times 10^3$) showed a significant difference in TH numbers compared with E35K and E57K (Fig. 2 *D* and *E*).

Consistent with the hypothesis that the oligomer-forming mutants are more toxic, E35K and E57K induced the largest TH-positive cell loss of all mutants studied. In summary, in the lentivirus PD rat model, the following ranking scale from toxic to nontoxic could be determined: E57K > E35K ≥ A30P ≥ E46K ≥ hWT α-syn > A53T ≥ α-syn(30–110) ≥ GFP only. A comparison of brain tissue stained for the panneuronal marker (NeuN) and TH revealed that, despite a significant loss of NeuN-positive cells (Fig. S3*A*), numerous nondopaminergic neurons survived inside the lesioned area of the SN, indicating that the loss was more severely affecting dopaminergic neurons. The percentage of TH-positive cells among NeuN-positive cells was approximately 75% in controls and decreased to 67% in hWT α-syn and 61% in the E57K group (Fig. S3 *A* and *C*).

A more detailed analysis of the effect of α-syn variants in the rat SN showed that E57K could lead to severe changes in neuron morphology compared with hWT α-syn (Fig. 2 *F–M*). Specifically, a dying back of neurites was observed in the E57K group (Fig. 2*H*), resembling the axonal pathology described in PD (24, 25). In addition, the neurites contained larger lump-like appearances within the E57K group than in the hWT α-syn (Fig. 2 *K* and *M*).

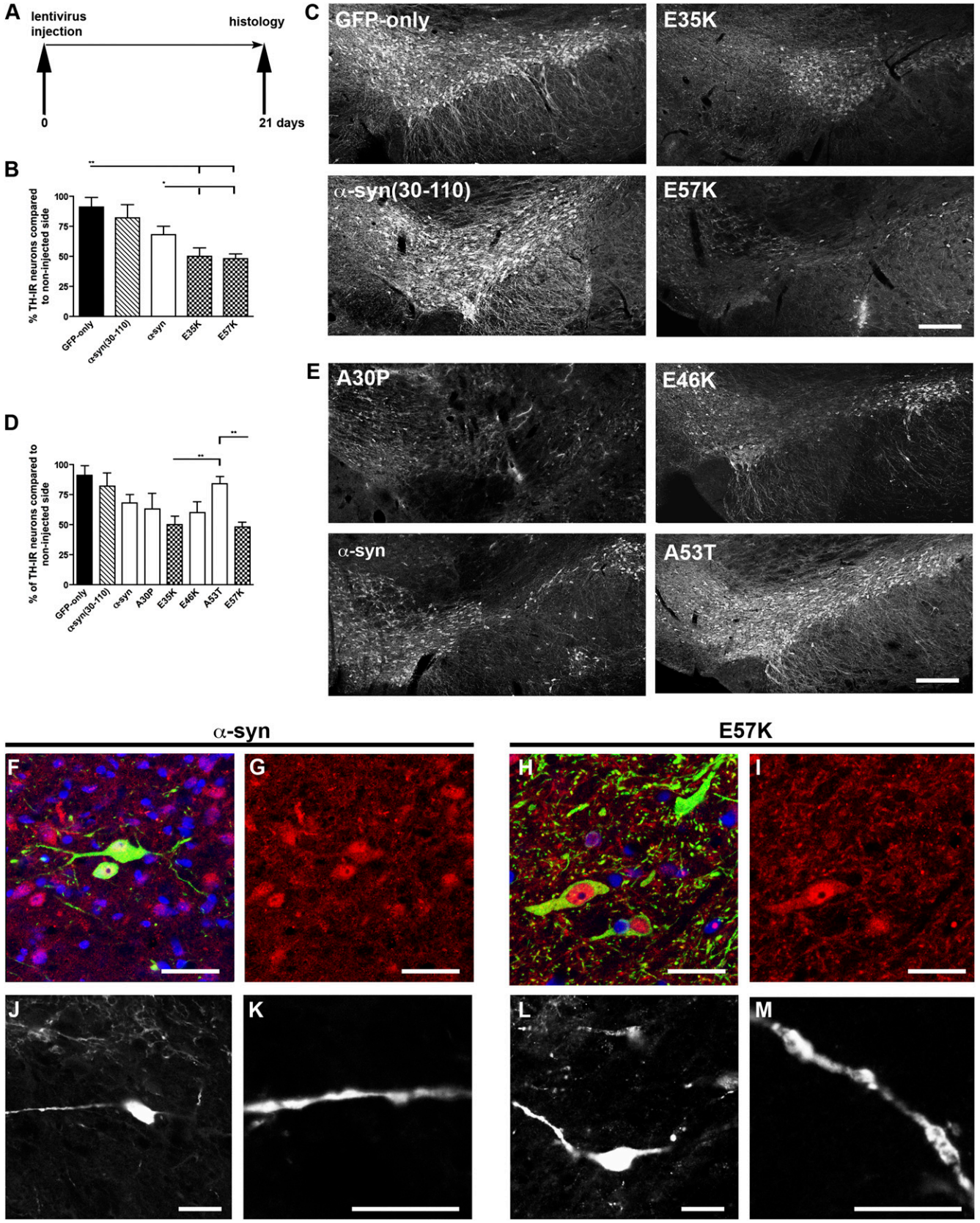

Fig. 2. Toxicity of hWT α-syn and α-syn variants in the SN of lentivirus-injected rats. (*A*) Injection paradigm: rats unilaterally injected with the different lentiviral constructs in the SN. (*B*) Histograms representing the decrease in numbers of TH-immunoreactive (TH-IR) neurons in the SN relative to the contralateral side, as evaluated by stereology. The nigral dopaminergic neurons were labeled with TH (*C* and *E*). Note that the loss of TH-expressing cells caused by α-syn variant expression was more pronounced close to the injection site (*C* and *E*). (*B*) Histogram representing the percentage of TH-positive neurons compared with the noninjected side. The artificial mutants E35K and E57K led to a significant decrease in TH-positive cells (**$P < 0.001$ vs. GFP and *$P < 0.05$ vs.

The expression levels of the α-syn variants encoded by the various lentiviral vectors were found to be similar by Western blot analysis in 293T cells (Fig. S3*F*). Based on the expression analysis of human α-syn (Fig. S3*G*), the injected virus diffused from each of two predetermined injection sites around the SN region.

The presented rat lentivirus model is in part artificial not only because lentivirus encoding human α-syn variants is locally injected into rat brains but also because α-syn is potentially overexpressed. Under the CMV promoter used earlier, we estimated that gene overexpression of human α-syn in comparison with endogenous α-syn is approximately eightfold higher in microdissected rat SN (Fig. S4*A*). By using the weaker promoter, EF1α, the overexpression could be lowered considerably; however, it still exceeded the expression levels in cases of familial PD presenting a triplication in the α-syn gene (5) (Fig. S4*A*). To test whether, even at such lowered expression levels, E57K is more toxic than hWT α-syn, SN TH-positive neurons were quantified in rats 3 and 9 wk after injection into the right SN of virus expressing E57K or hWT α-syn under the EF1α promoter (Fig. S4 *C–F*). At 3 wk, only minimal toxicity was observed for both E57K and hWT α-syn, whereas at 9 wk, an increased toxicity for the E57K variant was observed compared with hWT α-syn (Fig. S4 *C–F*). This experiment further indicates that E57K is more toxic to dopaminergic neurons than hWT α-syn. In addition, it highlights a time-dependent and an expression level-dependent effect of α-syn toxicity.

Another important issue is whether the observed toxicity of α-syn variants is specific or whether any protein aggregate expressed at high levels might be toxic in vivo (26). To further strengthen this argument, a lentiviral construct encoding the prion domain (aa 218–289) of the HET-s prion protein from the fungus *Podospora anserina*, which forms infectious, nontoxic amyloid-like aggregates, was generated (27). No significant changes in TH cell numbers were noticed when the HET-s lentivirus was introduced into the rat SN, indicating that the HET-s aggregates were also not toxic to dopaminergic neurons (Fig. S4*B*).

Toxicity of hWT α-Syn and α-Syn Variants in Cell-Based Assays. To test if the mutants that favor oligomer formation compared with the mutants that form fibrils are more quickly toxic in a cell-based system, we investigated cell death in a human mesencephalic immortalized neuronal cell line [Lund human mesencephalic (LUHMES) cells (28)] infected with the α-syn lentivirus. The percentage of activated caspase-3/DAPI–positive cells was analyzed. In the E35K and E57K groups (Fig. S5*A*, *D*, and *E*), the percentages of activated caspase-3/DAPI–positive cells were 11.2% and 9.5%, respectively. We compared E35K and E57K versus the mutants that form fibrils faster and found that the increase in cell death in both oligomerizing mutants was significantly higher than the increase in cell death in α-syn (Fig. S5*C*), E46K, and A53T (Fig. S5*A*). α-Syn(30–110) did not lead to a significant increase in cell death compared with the GFP-only group (Fig. S5*B*; $P > 0.05$).

The calcium influx assay had been previously established to monitor toxicity of α-syn oligomers (9). We asked if an increased calcium influx was present in the oligomerizing mutants E57K and E35K compared with the mutants that form fibrils faster. In differentiated LUHMES cells, we found that the most toxic mutant was E57K, followed by E35K. Calcium influx in the two oligomer-forming mutants was significantly higher than in α-syn and in the familial mutants E46K and A53T (Fig. S5*F*), which is indicative of cellular dysfunction caused by a stronger impact by E35K and E57K. There was no significant difference calcium influx between α-syn(30–110) and GFP only. The increased toxicity in E35K and E57K was further substantiated by a significant increase in cell viability, as measured by a calcein assay. Compared with α-syn and the familial mutants, the decrease in viable cells was significant in E35K and E57K compared with all other groups (Fig. S5*G*). Taken together, the results of activated caspase-3 counts, calcium influx assay, and calcein assay indicated that the oligomer-forming mutants were more toxic than the mutants that formed fibrils faster. Specifically, these findings suggest that the oligomerizing mutants E35K and E57K interfere more strongly with membranes than the other α-syn mutants analyzed.

α-Syn Interaction with Membranes. As our cell-based assays suggested that oligomer-forming mutants might be involved in the disruption of membranes, we next studied the interaction of the oligomer-promoting mutant E57K with organic lipids and membranes. Ultrastructural studies were performed on recombinant α-syn protein preparations that had been incubated with lipid monolayers [according to a previously published study (9)]. EM analysis showed that E57K mutants promoted the formation of more ring-like structures when incubated with the lipid monolayer in comparison with α-syn (Fig. S6*C*, protocol C). In this system, A30P and α-syn(30–110) did not form ring-like aggregates at all.

In another experiment, the binding of α-syn variants to vesicles made of brain-derived lipids (i.e., polar extract) and phosphatidylglycerol was investigated by liposome pull-down assays (Fig. S6 *A* and *B*, respectively, protocol C). In agreement with previous reports, α-syn had a binding preference for anionic vesicles (29, 30). Similar to the aforementioned lipid monolayer experiment, and in agreement with previous reports (31), A30P had a low affinity to both types of liposomes, which was attributed to a possible disruption of the N-terminal helix that forms upon protein binding to liposomes. The lack of the 29 N-terminal residues of α-syn might also account for the low binding of α-syn (30–110). In conclusion, the more toxic oligomerizing mutants, E35K and E57K, displayed a slightly higher affinity to bind liposomes in comparison with hWT α-syn, which might be indicative of a stronger reactivity with membranes.

Immunoblot Analysis of Aggregated α-Syn from Lentivirus-Injected Brains. The toxicity of α-syn depends on the interaction with membranes and lipids. As the oligomer-forming mutants are more toxic and membrane binding than the mutants that form fibrils more quickly, we next studied the mobility of the different α-syn mutants.

We performed immunoblot analysis on microdissected rat SN extracted 1 wk after lentivirus injection. SDS-stable α-syn oligomers, including dimers, trimers, and pentamers, were present in the membrane fractions [Fig. 3*A*; note that quantitative Western blot analysis of α-syn(30–110) was not possible because of the lack of a comparable antibody]. In particular, in E35K and E57K, the α-syn trimers in the membrane fraction were more abundant compared with hWT α-syn (Fig. 3 *A* and *B*). These results could also be confirmed with the use of a later time point (3 wk), when E57K showed more SDS-stable oligomers than hWT α-syn (Fig. S7*D*). As expected, no significant differences were found in the soluble fractions, in which mainly monomers were present (Fig. S7 *A–C*), indicating that the oligomers were mostly found in the membrane fraction. When comparing toxicity as analyzed by dopaminergic cell loss and the presence of the trimer bands, increased cell loss was observed in the mutants that had the largest number of trimers (Fig. 3*C*). To further characterize the different multimer fractions, we com-

hWT α-syn in *B* and *C*). In contrast, no significant loss of TH expression was observed with the lentivirus encoding for α-syn(30–110). (Values refer to means ± SD; $n = 4$ animals per group). (Scale bars: 250 μm in *C* and *E*.) (*D*) Overexpression of the familial variants A30P and E46K significantly decreased the number of TH-immunoreactive neurons. E35K and E57K were significantly decreased compared with A53T (*$P < 0.001$). (*E*) Representative brain slices showing the α-syn variants A30P, E46K, A53T, and hWT α-syn. (*F–M*) Examples of TH/α-syn double-positive cells shown in the hWT α-syn (*F–I*) and E57K group (*J–M*) 1 wk after lentiviral injection. Note the different TH morphology (green staining in *F* and *H*) in the hWT α-syn group, TH-positive cells with extended processes are visible (*F* and *H*: merged images; TH staining, green; α-syn staining, red; DAPI, blue). (*G* and *I*) α-Syn staining in red. In the E57K group, only the cytoplasm of TH-positive cells is visible, but their processes are rare. Some α-syn–positive cells colabel with TH. (*J*, *K*, *L*, and *M*) In addition, a difference in the morphology of the dendrites of α-syn–positive neurons (TH-negative) was noticed, with larger clumping of the dendrites in the E57K group. (Scale bars in *F–M*: 20 μm.)

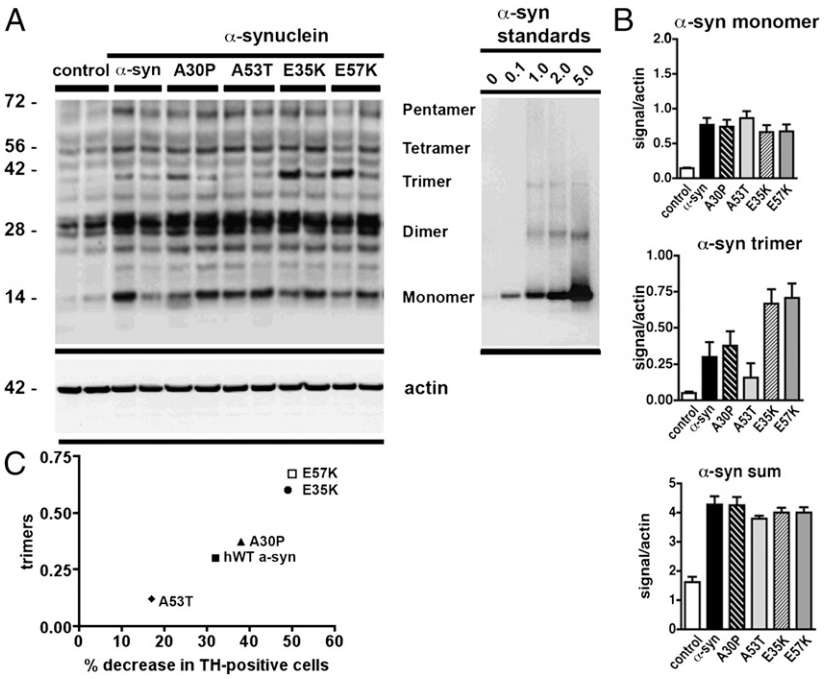

Fig. 3. Immunoblot analysis of aggregated α-syn from recombinant protein and lentivirus-injected brains. Representative Western blots (*A*) depict the insoluble fraction of microdissected SN for the different groups indicated after ultracentrifugation. Protein samples (20 μg) from two animals per group were run on denaturing polyacrylamide gels along with the indicated amounts (in ng) of purified recombinant hWT α-syn (protocol C). Blots were probed with an anti–α-syn antibody (*Upper*) and an anti-actin antibody (*Lower*) as loading control. The position of protein size markers (in kDa) is shown (*Left*). Note that, in the insoluble fraction, extensive oligomeric bands are present in the E57K mutant (*A*), whereas mostly monomers are present in the soluble fraction. Quantitative ECL analysis with a Versadoc imaging system that allows acquisition of data within a dynamical linear range (*B*) revealed a significant increase in the number of trimers in the insoluble fraction of α-syn (*B*). The ratio is calculated based on the actin loading and the immunoreactivity of the recombinant protein (h-WT α-syn). (*C*) Structure–toxicity relationship of α-syn: correlation between percent decrease in TH-positive cells in the SN upon lentiviral injection of α-syn variants (*x* axis) and relative number of in vivo-derived trimers detected by Western blot (*y* axis). Interestingly, a comparison between the 1-wk (Fig. 3*A*) and 3-wk time points (Fig. S7*D*) indicated that the size of the SDS-stable oligomers appeared to be time-sensitive.

pared recombinant protein (protocol A) and microdissected SN after performing a SEC. By probing the fraction from the SEC that in the previous characterization of A11-responsive oligomers had shown multimer bands (Fig. S2) with an α-syn antibody (Fig. S8), we observed multimer bands under denaturing and native conditions. Multimer bands were present under denaturing and native conditions (Fig. S8*B*). Similar to the recombinant material (Fig. S8*B*), SDS-stable α-syn monomer and multimers were present in the void peak (fraction 16) of SEC of brain tissue infected with E57K (Fig. S8 *C* and *D*). Hence, α-syn oligomers composed of SDS-stable multimers were present in a cell-free system, where they formed ring-like aggregates, and in vivo (Fig. S8 *C* and *D*).

In conclusion, we have generated mutants that favored oligomerization and compared them with mutants that formed fibrils more quickly. In vivo, the mutants that favored oligomerization induced increased dopaminergic loss (Fig. 2) and neuronal cell death. The increased calcium influx is indicative of stronger interactions with cell membranes (Fig. S5). Furthermore, the mutants that favored oligomerization strongly bound to lipid membranes and showed multimers when immunoblotted (Fig. S6).

Discussion

It has been proposed that prefibrillar oligomers, as opposed to mature fibrils, may represent the toxic species in PD (21, 32). Although the presence of such annular protofibrils in vitro has been shown to alter membrane permeability, evidence of the toxicity of oligomers in mammalian systems is still limited (11, 12). To address this issue, both fibril-promoting and oligomer-forming variants of α-syn were designed and analyzed biophysically, and their in vivo toxicity was investigated. Under certain in vitro circumstances, both recombinant E35K and E57K variants formed pronounced ring/pore-like structures, in contrast to hWT α-syn, familial mutants, and the fibril-promoting variant α-syn (30–110) (Fig. 1).

In vivo, following lentiviral injection into the rat SN, we observed a decrease in dopaminergic cells in the rat SN, most prominently for E57K and E35K, followed by the familial mutants A30P, E46K, and hWT α-syn; in contrast, α-syn(30–110) did not show any significant toxic effect (Fig. 2 *A*–*E*). To strengthen the observed qualitative correlation between in vitro oligomerization and in vivo toxicity, immunoblot analysis was performed with dissected rat brain tissues 1 wk after lentivirus injection. In the membrane fractions, SDS-stable α-syn trimers were more abundant in E35K- and E57K-treated animals compared, for example, with hWT α-syn–infected animals (Fig. 3 *A* and *B*). As expected, no significant differences were observed among the various variants in the soluble fractions (Fig. S7 *A*–*C*). Overall, these findings indicate that the toxicity observed in the rat synuclein model used is related to a membrane-associated α-syn oligomer, with the mechanism of toxicity being linked to alterations in the permeability and integrity of the cell membrane. In cell-based systems, the oligomer-forming variant E57K induced high toxicity. In particular, an increase in cell death and Ca^{2+} influx and a decrease in cell viability, indicative of cellular and membrane dysfunction, were observed in a neuronal cell line (Fig. S5).

Both designed variants also displayed stronger reactivity to the oligomer-specific antibody A11 (22) than hWT α-syn (shown for E57K in Fig. S2). Starting with monomer entities, within 1 wk both variants showed the accumulation of large oligomeric intermediates, in contrast to hWT α-syn, familial mutants, and α-syn(30–110) (Fig. 1*C*). In the presence of membranes, within a few hours, E57K formed considerably more ring-like aggregates than hWT α-syn, the familial mutants studied, and the fibril-promoting variant α-syn(30–110) (Fig. S6*C*). In summary, under various in vitro conditions, both the E35K and E57 variants appeared to promote α-syn oligomer formation more prominently than hWT α-syn and the familial mutants, whereas α-syn (30–110) formed fibrils more quickly (Fig. 1 and Figs. S1 and S6).

Although, to our knowledge, this is the first report to directly link (artificial) membrane-associated α-syn oligomers to an increased loss of nigral TH-positive neurons in a murine model, the presented findings are in line with previous data. There is enhanced formation of oligomers in PD (33); in vitro α-syn oligomers may interact with lipids and may disrupt or perforate membranes (7–9, 21, 11) and cause cell death in cell systems (10, 11) and in nonmammalian models, such as *C. elegans* and *D. melanogaster* (12). In addition, an increased release via vesicle-mediated exocytosis, specifically for misfolded and damaged α-syn, probably by exosomes in a calcium-dependent manner (34), has been described (reviewed in ref. 35). Combining the presented in vitro and in vivo experiments with our published work on the potential toxicity of α-syn multimers (9), we suggest that the in vivo-derived SDS-stable multimers may be the building blocks for larger α-syn oligomers and that these species

cause toxicity by aggregation to the cell membrane. Not all prefibrillar oligomeric species that are present are annular or ring-like; therefore, there might be other oligomeric species present and potentially involved in increasing toxicity.

In conclusion, the presented structure–toxicity relationship study of human α-syn supports the notion that amyloid fibrils are not directly toxic, despite being present in the LBs, which are the pathological hallmark of PD. Our findings implicate large α-syn oligomers as the toxic species in PD. The model created here will be an important tool to further understand the downstream effects and molecular basis of oligomerization in synucleinopathies and to develop effective therapeutic strategies.

Methods

Recombinant Protein Expression. The hWT α-syn expression plasmid was a gift of M. Goedert (University of Cambridge, Cambridge, United Kingdom). The α-syn variants α-syn(30–110), A30P, E35K, E46K, A53T, E57K, E61K, and E83K were constructed by site-directed mutagenesis (QuikChange kit; Stratagene) and the mutations were confirmed by DNA sequencing. The detailed preparations are described in *SI Methods*.

Lentiviral Vectors and Virus Preparation. DNA fragments containing the hWT α-syn coding sequence (nucleotides 47–469 of GenBank accession no. NM_000345) and variants were obtained by PCR from the corresponding *Escherichia coli* expression plasmids (as described earlier) and cloned by restriction enzymes AgeI and PstI into the lentiviral transfer vector IRES-GFP containing an internal ribosome entry site–GFP sequence located downstream of the α-syn gene. In this third-generation lentiviral vector, the CMV promoter constitutively drives the expression of both α-syn and GFP.

Stereotaxic Injection and Tissue Preparation. Lentiviral particles (estimated as 1.5×10^8 U/mL) were stereotaxically injected in the right SN of adult (age 3 mo) female Fisher F344 rats (Harlan Laboratories) weighing approximately 200 g as previously described (23). In brief, viral suspensions (2 μL volumes) were injected with a 10 μL Hamilton syringe at a rate of 0.2 μL/min. Stereotaxic injections were delivered to two sites within the SN with the following coordinates: anteroposterior, −4.8 mm, mediolateral, −2 mm, dorsoventral, −8.2 mm; and anteroposterior, −5.5 mm, mediolateral, −1.7 mm, and dorsoventral, −8.2 mm, respectively, from bregma. Further information is provided in *SI Methods*.

Tissue Culture Experiments. LUHMES cells were used for tissue culture experiments. They are a conditionally immortalized human neuronal cell line and were a gift from M. Leist and D. Schols (28). The LUHMES cells were maintained as described previously under a proliferative state with FGF-2 or under neuronal differentiation conditions (28). Activated caspase-3 cell counts, calcein assay, and calcium influx assay are described in detail in *SI Methods*.

Immunoblot Analysis. To analyze the distribution and levels of α-syn in the brains of rodents injected with the lentiviral particles, as previously described, samples were lysed and extracts fractioned into soluble and insoluble fractions by ultracentrifugation (25). Twenty micrograms of protein per lane were loaded into 4% to 12% SDS/PAGE gels and blotted onto PVDF membranes. Membranes were incubated with rabbit polyclonal anti–α-syn (1:1,000; Chemicon; Fig. 3 and Fig. S7) or mouse monoclonal α-syn antibody (1:1,000; BD; Fig. S8) antibody, followed by secondary antibodies tagged with HRP (1:5,000; Santa Cruz Biotechnology), and bands were visualized by enhanced chemiluminescence and analyzed with a quantitative Versadoc XL imaging apparatus (BioRad) that allows acquisition of data within a dynamic linear range. Actin was used as a loading control. Immunoreactivity of the recombinant protein was calculated relative to the actin signal (9).

ACKNOWLEDGMENTS. We thank B. Miller, E. Meija, S. Schroeter, and C. Patrick for excellent technical support. We thank M. Goedert for the hWT α-syn plasmid, O. Singer for the EF1a plasmid, and M. Leist and D. Schols for the LUHMES cells. We thank O. Bracko, J. Winkler, and K. Danzer for helpful discussions and M. L. Gage for editing the manuscript. This work was supported in part by the National Institutes of Health, the Swiss National Foundation, the California Institute for Regenerative Medicine, the Picower Foundation, the Lookout Fund, the Michael J. Fox Foundation, and the Alexander von Humboldt Foundation.

1. Fearnley JM, Lees AJ (1991) Ageing and Parkinson's disease: Substantia nigra regional selectivity. *Brain* 114:2283–2301.
2. Goedert M (2001) Alpha-synuclein and neurodegenerative diseases. *Nat Rev Neurosci* 2:492–501.
3. Polymeropoulos MH, et al. (1996) Mapping of a gene for Parkinson's disease to chromosome 4q21-q23. *Science* 274:1197–1199.
4. Zarranz JJ, et al. (2004) The new mutation, E46K, of alpha-synuclein causes Parkinson and Lewy body dementia. *Ann Neurol* 55:164–173.
5. Singleton AB, et al. (2003) alpha-Synuclein locus triplication causes Parkinson's disease. *Science* 302:841.
6. Krüger R, et al. (1998) Ala30Pro mutation in the gene encoding alpha-synuclein in Parkinson's disease. *Nat Genet* 18:106–108.
7. Conway KA, Harper JD, Lansbury PT (1998) Accelerated in vitro fibril formation by a mutant alpha-synuclein linked to early-onset Parkinson disease. *Nat Med* 4:1318–1320.
8. Conway KA, Harper JD, Lansbury PT, Jr. (2000) Fibrils formed in vitro from alpha-synuclein and two mutant forms linked to Parkinson's disease are typical amyloid. *Biochemistry* 39:2552–2563.
9. Tsigelny IF, et al. (2008) Mechanisms of hybrid oligomer formation in the pathogenesis of combined Alzheimer's and Parkinson's diseases. *PLoS ONE* 3:e3135.
10. Caughey B, Lansbury PT (2003) Protofibrils, pores, fibrils, and neurodegeneration: Separating the responsible protein aggregates from the innocent bystanders. *Annu Rev Neurosci* 26:267–298.
11. Danzer KM, et al. (2007) Different species of alpha-synuclein oligomers induce calcium influx and seeding. *J Neurosci* 27:9220–9232.
12. Karpinar DP, et al. (2009) Pre-fibrillar alpha-synuclein variants with impaired beta-structure increase neurotoxicity in Parkinson's disease models. *EMBO J* 28:3256–3268.
13. Heise H, et al. (2005) Molecular-level secondary structure, polymorphism, and dynamics of full-length alpha-synuclein fibrils studied by solid-state NMR. *Proc Natl Acad Sci USA* 102:15871–15876.
14. Vilar M, et al. (2008) The fold of alpha-synuclein fibrils. *Proc Natl Acad Sci USA* 105:8637–8642.
15. Serpell LC, Berriman J, Jakes R, Goedert M, Crowther RA (2000) Fiber diffraction of synthetic alpha-synuclein filaments shows amyloid-like cross-beta conformation. *Proc Natl Acad Sci USA* 97:4897–4902.
16. Chen M, Margittai M, Chen J, Langen R (2007) Investigation of alpha-synuclein fibril structure by site-directed spin labeling. *J Biol Chem* 282:24970–24979.
17. Der-Sarkissian A, Jao CC, Chen J, Langen R (2003) Structural organization of alpha-synuclein fibrils studied by site-directed spin labeling. *J Biol Chem* 278:37530–37535.
18. Petkova AT, et al. (2002) A structural model for Alzheimer's beta -amyloid fibrils based on experimental constraints from solid state NMR. *Proc Natl Acad Sci USA* 99:16742–16747.
19. Lührs T, et al. (2005) 3D structure of Alzheimer's amyloid-beta(1-42) fibrils. *Proc Natl Acad Sci USA* 102:17342–17347.
20. Lashuel HA, Hartley D, Petre BM, Walz T, Lansbury PT, Jr. (2002) Neurodegenerative disease: Amyloid pores from pathogenic mutations. *Nature* 418:291.
21. Conway KA, et al. (2000) Acceleration of oligomerization, not fibrillization, is a shared property of both alpha-synuclein mutations linked to early-onset Parkinson's disease: Implications for pathogenesis and therapy. *Proc Natl Acad Sci USA* 97:571–576.
22. Kayed R, et al. (2003) Common structure of soluble amyloid oligomers implies common mechanism of pathogenesis. *Science* 300:486–489.
23. Lo Bianco C, Ridet JL, Schneider BL, Deglon N, Aebischer P (2002) alpha-Synucleinopathy and selective dopaminergic neuron loss in a rat lentiviral-based model of Parkinson's disease. *Proc Natl Acad Sci USA* 99:10813–10818.
24. Galvin JE, Uryu K, Lee VM, Trojanowski JQ (1999) Axon pathology in Parkinson's disease and Lewy body dementia hippocampus contains alpha-, beta-, and gamma-synuclein. *Proc Natl Acad Sci USA* 96:13450–13455.
25. Chung CY, Koprich JB, Siddiqi H, Isacson O (2009) Dynamic changes in presynaptic and axonal transport proteins combined with striatal neuroinflammation precede dopaminergic neuronal loss in a rat model of AAV alpha-synucleinopathy. *J Neurosci* 29:3365–3373.
26. Gidalevitz T, Ben-Zvi A, Ho KH, Brignull HR, Morimoto RI (2006) Progressive disruption of cellular protein folding in models of polyglutamine diseases. *Science* 311:1471–1474.
27. Ritter C, et al. (2005) Correlation of structural elements and infectivity of the HET-s prion. *Nature* 435:844–848.
28. Schildknecht S, et al. (2009) Requirement of a dopaminergic neuronal phenotype for toxicity of low concentrations of 1-methyl-4-phenylpyridinium to human cells. *Toxicol Appl Pharmacol* 241:23–35.
29. Davidson WS, Jonas A, Clayton DF, George JM (1998) Stabilization of alpha-synuclein secondary structure upon binding to synthetic membranes. *J Biol Chem* 273:9443–9449.
30. Volles MJ, et al. (2001) Vesicle permeabilization by protofibrillar alpha-synuclein: Implications for the pathogenesis and treatment of Parkinson's disease. *Biochemistry* 40:7812–7819.
31. Bussell R, Jr., Eliezer D (2004) Effects of Parkinson's disease-linked mutations on the structure of lipid-associated alpha-synuclein. *Biochemistry* 43:4810–4818.
32. Conway KA, et al. (2000) Accelerated oligomerization by Parkinson's disease linked alpha-synuclein mutants. *Ann N Y Acad Sci* 920:42–45.
33. Sharon R, et al. (2003) The formation of highly soluble oligomers of alpha-synuclein is regulated by fatty acids and enhanced in Parkinson's disease. *Neuron* 37:583–595.
34. Emmanouilidou E, et al. (2010) Cell-produced alpha-synuclein is secreted in a calcium-dependent manner by exosomes and impacts neuronal survival. *J Neurosci* 30:6838–6851.
35. Kim C, Lee SJ (2008) Controlling the mass action of alpha-synuclein in Parkinson's disease. *J Neurochem* 107:303–316.